Deletions in a *dSpm* Insert in a Maize *bronze-1* Allele Alter RNA Processing and Gene Expression

Victor Raboy,[1] Hwa-Yeong Kim,[2] John W. Schiefelbein[3] and Oliver E. Nelson, Jr.

Laboratory of Genetics, University of Wisconsin, Madison, Wisconsin 53706

Manuscript received October 8, 1988
Accepted for publication April 10, 1989

ABSTRACT

The *bz-m13* allele of the *bronze-1* (*bz*) locus in maize contains a 2.2-kb *defective Suppressor-mutator* (*dSpm*) transposable element inserted in the second exon. We compared *bz* expression in *bz-m13* and five derivatives in which the *dSpm* insertion had sustained deletions ranging from 2 to 1300 bp. Tissues homozygous for *bz-m13* in the absence of *Spm-s* activity were found to contain from 5 to 13% of the enzymatic activity conditioned by a wild-type allele at the *bz* locus. Tissues homozygous for the deletion derivatives contained enzymatic activities ranging from less than 1% to 67%. These differences are closely correlated with the steady-state level of one of two alternatively spliced transcripts. In all alleles *bz* transcription proceeds through the *dSpm* insert. Subsequent RNA processing uses the donor site of the single *bz* intron and either one of two alternative acceptor splice sites (AS1 and AS2) located within the *dSpm* sequence. Use of the AS1 removes all but 2 bp of *dSpm* sequence and produces the 1.8-kb transcript whose level corresponds closely to the level of enzymatic activity. Use of AS2 produces a transcript which retains more than 600 bp of *dSpm* sequence. Those derivatives in which AS2 is either deleted or inactivated have substantially increased levels of both the 1.8-kb transcript and enzymatic activity. We therefore document one sequence of events which began with the insertion of a transposable element and resulted in novel and stable introns which retain element-derived sequence and which in certain cases permit substantial host-gene expression.

RECENT studies have shown that in certain cases maize (*Zea mays* L.) transposable element insertions in structural genes do not alter the structural gene's transcription initiation site, and that transcription proceeds through the transposable element insertion. Most or all of the transposable element sequence is then removed from the primary transcript using either donor or acceptor splice sites which are found within the transposable element sequence but are not part of a known transposable element gene (DENNIS *et al.* 1988; KIM *et al.* 1987; SIMON and STARLINGER 1987; WESSLER, BARAN and VARAGONA 1987). These studies have demonstrated that maize transposable element insertions can in certain cases alter the intervening sequence of a structural gene.

The *Suppressor-mutator* (*Spm*) family of transposable elements in maize consists of autonomous transposition-competent *Spm* elements and nonautonomous transposition-defective *Spm* (*dSpm*) elements, which can be excised from a locus only in the presence of an active *Spm* (MCCLINTOCK 1954, 1955; FEDOROFF 1983). PETERSON (1953, 1960) independently characterized the *Enhancer* (*En*) transposable element, which he showed to be genetically equivalent to *Spm* (PETERSON, 1965), and which subsequently was found to be nearly identical in sequence to *Spm* (PEREIRA *et al.* 1986; MASSON *et al.* 1987). MCCLINTOCK (1954) found that the association of *dSpm* elements with structural genes can in certain cases permit nonmutant phenotypes in the absence of *Spm* activity.

NELSON and KLEIN (1984) reported the isolation of a *dSpm* insertion mutation of this type in the *bronze-1* (*bz*) locus in maize, termed *bz-m13*. Functional *Bronze* (*Bz*) alleles at the *bz* locus encode the enzyme UDP glucose:flavonoid 3-*O*-glucosyltransferase (UFGT, EC 2.3.1.91), which catalyzes a late step in the anthocyanin biosynthetic pathway (LARSON and COE 1977; DOONER and NELSON 1977a). The *bz-m13* allele contains a 2.2-kb *dSpm* insertion in the second exon of the *bz* gene, 38 bp downstream of the 3′ end of the single *bz* intron (SCHIEFELBEIN *et al.* 1988). In the absence of an active, standard *Spm* (*Spm-s*), the accumulation of anthocyanin pigment in the aleurone layer of kernels homozygous for *bz-m13* is indistinguishable from that of a *Bz* allele, but a reduced level of UFGT activity is recovered from endosperm extracts (KLEIN and NELSON 1983).

In the presence of an active *Spm-s*, the *dSpm* insertion in *bz-m13* frequently undergoes mutation prior to or during both male and female gametogenesis, often resulting in high germinal mutation rates (NEL-

[1] Present address: USDA-ARS, Department of Plant and Soil Science, Montana State University, Bozeman, Montana 59717.
[2] Present address: Alpine Experiment Station, #1 Hoinggye-ri, Doammyeon, Pyeongchang-gun, Gangwon-do 232-950, Republic of Korea.
[3] Present address: MSU-DOE Plant Biology Laboratory, Michigan State University, East Lansing, Michigan 48824.

SON and KLEIN 1984). The majority of these mutations (up to 83% of a progeny family) represent excision of the *dSpm* resulting in stable functional (*Bz'*) or nonfunctional (*bz'*) derivatives (NELSON and KLEIN 1984; SCHIEFELBEIN *et al.* 1988). A small fraction of germinal mutations result in novel unstable derivatives of *bz-m13*. These derivatives differ from *bz-m13* in their *Spm*-induced pattern of somatic reversion. MCCLINTOCK (1968) termed such derivatives "changes-in-state" (CS). Six CS derivatives of *bz-m13* have been described (SCHIEFELBEIN *et al.* 1985). Aleurone pigmentation in these six CSs in the absence of *Spm-s* is indistinguishable from that of the initial state of *bz-m13*. A molecular analysis of these six CSs revealed that the site of *dSpm* insertion has not changed (SCHIEFELBEIN *et al.* 1985). Five of the six CSs contained deletions within the 2.2-kb *dSpm* insert.

One of these, *bz-m13 CS9* (*CS9*), conditions 40–50% of *Bz* UFGT activity in the absence of *Spm-s* (KIM *et al.* 1987). This relatively substantial level of enzymatic activity is made possible by the fact that all but 2 bp of *CS9 dSpm* sequence is efficiently spliced out of the initial transcript as part of a novel intron. The splicing event utilizes the donor site of the single *bz* intron and an acceptor splice site located within the 13 bp *dSpm* terminal inverted repeat. Here we compare gene expression in *bz-m13* and the five deletion derivatives. We document a multi-step sequence of events that began with the insertion of a transposable element and resulted in novel, stable intron structures which in certain cases such as *CS9* permit substantial host-gene expression.

MATERIALS AND METHODS

Plant materials: The isolation of the initial *dSpm* insertion in the *bz* locus, *bz-m13*, was previously described (NELSON and KLEIN 1984). The five CS deletion derivatives of *bz-m13* included in this study are designated *bz-m13 CS3*, *bz-m13 CS5*, *bz-m13 CS6*, *bz-m13 CS9*, and *bz-m13 CS12* (abbreviated as *CS3*, *CS5*, etc.), and their isolation was previously described (SCHIEFELBEIN *et al.* 1985). The following *bz* alleles were used as controls or for comparative purposes: *bz-R*, the null reference allele; *bz-x2*, a deletion of the *bz* locus kindly provided by J. MOTTINGER; *Bz'3*, a functional derivative of *bz-m13* in which the *dSpm* and the 3 bp host-sequence duplication created upon its insertion have been perfectly excised (SCHIEFELBEIN *et al.* 1988); *Bz-McC*, a functional allele isolated from a stock provided by B. MCCLINTOCK; *Bz-W22*, a functional allele isolated from the W22 background; *Bz-McC2*, the functional allele extracted from the stock used in the isolation of *bz-m13*, and thus its progenitor allele. The molecular structure of *Bz'3*, *BzMcC2*, and *bz-m13* and its CSs was determined using both restriction mapping of genomic DNA and sequence analysis of genomic clones, as previously described (SCHIEFELBEIN *et al.* 1985, 1988).

At the onset of this study the *Bz-McC2* allele had not yet been extracted genetically from the *c-m5 Sh Bz wx-m8* stock utilized in the isolation of *bz-m13*. In an earlier report, the *Bz-McC* allele was used as a functional *Bz* control in comparisons with *bz-m13* (KLEIN and NELSON 1983). Subsequently, DNA sequence analysis revealed a number of differences between the *Bz-McC* allele and the *Bz* sequence common to the alleles in the *bz-m13* series (SCHIEFELBEIN 1987). Therefore, for biochemical comparisons we initially decided to use the *Bz'3* allele as a functional *Bz* control. Subsequently, *Bz-McC2* was isolated at the genetic and molecular levels and found to be indistinguishable from *Bz'3* (Table 2; SCHIEFELBEIN 1987).

All alleles used in this study originated in or were incorporated into the common background of the inbred W22. These stocks carry functional alleles at complementary loci necessary for anthocyanin synthesis in the aleurone (*A1*, *A2*, *Bz2*, *C1*, *C2*, *C1f*, *R*, and *Vp*) and are homozygous for a given *bz* allele in the absence of an active *Spm-s*. For maximum *Bz* expression in husk tissue, stocks were constructed to carry the dominant alleles at the *booster* (*b*), and *purple plant* (*pl*) loci (GERATS *et al.* 1984).

UFGT extraction and assay: Individual ears carrying the above alleles were harvested from field-grown plants at maturity, shelled, and stored at room temperature. Husk tissues were harvested from field-grown plants 15 days after silk emergence and stored at −70°C. For preparation of crude extracts of mature endosperms, 10 kernels were allowed to imbibe for 20 to 40 minutes in distilled H_2O. The pedicel, germ and pericarp were removed, and the endosperms thus prepared were ground to pass through a 40 mesh screen in a Wiley Mill. Unless otherwise indicated, all subsequent steps were conducted at 4°C. The flour was then extracted in 7.5 ml extraction buffer [100 mM HEPES pH 7.5, 100 mM NaCl, 50 mg ml^{-1} Ag 1-X2 (Cl^-) anion exchange resin, 10 mM β-mercaptoethanol] for 1 hr with constant stirring. Extracts were then centrifuged (10,000 *g* for 10 min), and the supernatants were decanted through a small glass-wool pad. For preparation of crude extracts of husks, tissue samples were pulverized in liquid N_2, and crude extracts were prepared as above except that 1 g of tissue was extracted in 4-ml extraction buffer that contained 250 mg ml^{-1} Agl-X2 (Cl^-).

Assays of UFGT activity were conducted using the method of KLEIN and NELSON (1983). Crude extract (20 μl) was assayed in a total volume of 50 μl containing 25 mM HEPES (pH 7.5), 5 mM $CaCl_2$, 2% PEG 8000, 10 mM β-mercaptoethanol, 2 mM [^{14}C]UDPG (specific activity of 0.5 mCi mM^{-1}) and 5 mM quercitin (dissolved in ethyleneglycol monomethylether). Reactions were stopped after 30 min by the addition of 150 μl of ethyl acetate, and the mixtures centrifuged for 3 min in a microcentrifuge to separate phases. The reaction products in the ethyl acetate phase were separated by ascending paper chromatography on Whatman No. 1 as described (DOONER and NELSON 1977a, b), and the incorporation of [^{14}C]glucose into isoquercitrin was determined. All assays were conducted in duplicate. A unit of UFGT activity is defined as the synthesis of 1 μmol of isoquercitrin per hr.

Thermal stability profiles were conducted as previously described (DOONER and NELSON 1977b). Measurement of cross-reactive material (CRM) was conducted as previously described using polyclonal antibodies raised against partially purified *Bz-W22* endosperm UFGT (KLEIN and NELSON 1983).

RNA blot hybridization analysis: Total cellular RNA was extracted as described (FURTEK 1986) from the husk tissue preparations used for the UFGT assays described above. RNA samples (7 μg) enriched for polyadenylated [poly(A)$^+$]RNA were fractionated in 1.2% agarose/2.2 M formaldehyde gels, transferred to nitrocellulose filters, and probed with ^{32}P-labeled DNA.

S1 nuclease protection analysis: We used a modification of the procedures as previously described (BERK and SHARP 1977; FAVALORO, TREISMAN and KAMEN 1980). The optimum hybridization temperature was calculated using an equation for the determination of the melting temperature (Tm) of the probe DNA as described by CANTOR and SCHIMMEL (1980). Ten micrograms of poly(A)$^+$ RNA, 20 μg of calf liver RNA (Sigma type IV), and 1×10^4 cpm of 5′-end-labeled DNA fragment were coprecipitated, redissolved in 5 μl of hybridization solution [400 mM NaCl, 40 mM PIPES (pH 6.4), 1 mM EDTA, and 80% formamide], heated for 10 min at 85°C, and immediately placed in a water bath set at 70°. After 19 hr of incubation, 50 μl of S1 nuclease buffer [50 mM NaOAc (pH 5.5), 1 mM $ZnSO_4$, 300 mM NaCl, 10 μg ml^{-1} denatured Sigma calf thymus DNA] and 800 units ml^{-1} S1 nuclease (Pharmacia-PL) were added, and the reaction was incubated at 37°. The reaction was stopped after 1 hr by the addition of 14 μl of termination buffer (2.5 M NH_4OAc, 50 mM EDTA, 400 μg ml^{-1} Sigma *E. coli* tRNA). Nucleic acids were ethanol-precipitated, resuspended in formamide sample buffer, and fractionated in a 5% urea-polyacrylamide gel.

Assay of *dSpm* germinal excision rate: The genetic tests used here to assay rates of germinal excision of *dSpm* insertions, leading to the production of stable *Bz′* and *bz′* derivatives of *bz-m13*, follow those described by NELSON and KLEIN (1984). Briefly, plants of the genotype *Sh bz-m13/sh bz-r*; *+Spm-s* (indicating the genome contains at least one active *Spm-s* element) or *Sh bz-m13 CS/Sh bz-r*; *+Spm-s* were used as males and females in crosses with a tester stock of the genotype *sh bz-r*; *+Spm-s*. The germinal excision rate is calculated as the percentage of stable *Bz′* or *bz′* derivatives in the *bz-m13* progeny. *Sh* and *sh* are alleles of the *shrunken* locus, which is closely linked to the *bz* locus (2 map units). Homozygous *sh* endosperms display a characteristic shrunken phenotype, whereas one or more copies of *Sh* condition a wild-type, plump endosperm. The *Sh bz-m13* linkage is used here only to distinguish stable *Sh bz′* derivatives in the test-cross progeny from *sh bz-r* progeny.

In theory, every kernel in these test-cross progeny should contain at least one active *Spm-s*. In practice, a fraction of kernels contain no active *Spm-s*. Therefore, kernels displaying non-sectored anthocyanin pigmentation may represent either an allele of *bz-m13* in the absence of an active *Spm-s*, or a stable *Bz′* derivative, which is nonsectored in the presence or absence of an active *Spm-s*. To distinguish these genotypes, an active *Spm-s* was reintroduced in progeny tests of nonsectored kernels using bulked pollen of several *sh bz-r +Spm-s* tester stock plants. The use of bulked tester pollen ensures that the majority of kernels on a given test-cross ear will receive an active *Spm-s*, permitting clear distinction between an unchanged allele of *bz-m13* and a *Bz′* derivative.

RESULTS

Structure of the *bz-m13* alleles: A summary of our current knowledge (SCHIEFELBEIN *et al.* 1988) of the structures of the initial *dSpm* insertion mutation, *bz-m13*, and the five CSs included in this study are given in Figure 1. The 2.2 kb *dSpm* element in *bz-m13* is a deletion derivative of the full-length *Spm* (Figure 1a). This deletion removed 6045 bp of *Spm*'s internal sequence, but did not alter any of the element's terminal components. Thus the 2.2-kb *dSpm* retains the 13 bp terminal inverted repeats that are typical of elements in this family (SCHWARZ-SOMMER *et al.*

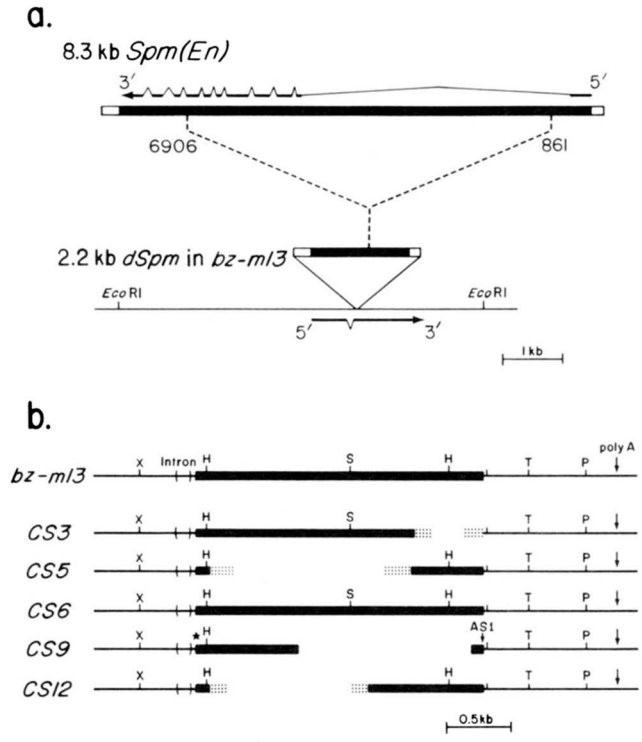

FIGURE 1.—Structure of *bz-m13* and its change-in-state (CS) derivatives. a) Structural relationship between the autonomous *Spm* (*En*) element and the *dSpm* element in *bz-m13*. The portion of the *Spm* element deleted in the *dSpm* element is noted by the dashed lines, and the coordinates are those of the *En-1* element (PEREIRA *et al.* 1986). The subterminal repetitive regions are indicated by the open portions of the bars. The structure of the major *Spm* (*En*) transcript (PEREIRA *et al.* 1986) is shown above the *Spm* element. The structure of the *Bz* gene transcript (FURTEK 1986) given under the structure of *bz-m13* indicates that the *dSpm* element is inserted in the second exon of the *Bz* gene and illustrates that the direction of transcription from the *Bz* promoter is opposite to the direction from the *Spm* (*En*) promoter. b) Structure of *bz-m13* and its CS derivatives. Open areas of *CS3*, *CS5*, *CS9*, and *CS12* indicate deletions of the *dSpm* sequence. Stippled areas represent regions of the *dSpm* elements where the exact deletion endpoints are unknown. The two bp deletion in the terminal inverted repeat of the *dSpm* in *CS6* is indicated by a star. AS1, pre-mRNA acceptor splice site identified within the terminal inverted repeat of *CS9*. Restriction enzyme sites: X, *Xma*I; H, *Hin*cII; S, *Sph*I; T, *Sst*I.

1984), the 180- and 299-bp "subterminal repetitive regions" (SRRs; MASSON *et al.* 1987; SCHWARZ-SOMMER *et al.* 1984) one of which contains the putative promoter for *Spm*'s major (gene 1) transcript (PEREIRA *et al.* 1986), and the GC-rich first exon of gene 1. The *dSpm* is inserted into the *bz* gene in opposite orientation in terms of the *bz* and *Spm* gene 1's directions of transcription. The five CSs were found to contain deletions within the 2.2-kb *dSpm* without a change in the position or orientation of the insert (Figure 1b; SCHIEFELBEIN *et al.* 1985, 1988). In *CS3* and *CS9* the deletions extend from internal sequences to within the 3′ SRR (5′ in terms of *Spm*'s direction of transcription). In *CS5* and *CS12* the deletions extend from internal sequences to within the 5′ SRR (3′ in terms of *Spm*'s direction of transcription). In CS6 the dele-

TABLE 1

Characteristics of UFGT isolated from mature endosperm and husk tissues[a] of *bz-m13* and its change in state derivatives

	Mature endosperm				Husk		
	Specific activity[b]				Specific activity[b]		
Allele	Units mg protein	% *Bz'3*	CRM[c] (% *Bz'3*)	Half-life at 55°[d] (min)	Units mg protein	% *Bz'3*	Half-life at 55°[d] (min)
Bz'3	451	100	100	9.9	990	100	44.5
Bz-McC2	467	104	85	7.9			
bz-m13	24	5	5	3.2	128	13	3.7
bz-m13 CS3	168	37	20	3.1	388	39	4.4
CS5	24	5	4	3.4	132	13	5.5
CS6	30	7	1	3.6	198	20	5.1
CS9	304	67	57	3.3	490	49	4.8
CS12	2	<1	<1		25	3	
Bz-McC	520	115	172	7.6			
Bz-W22	526	117	159	30.0			237.8
SE	30		28		75		

[a] Tissue was isolated from plants homozygous for the indicated *Bz* allele. The data represent the mean value for two replications consisting of individual plants. The standard deviation of the mean, or standard error, is given below each variable.

[b] A unit of UFGT activity is defined as a μmol of isoquercitrin formed per hour. With the methods used here, UFGT activity is not detectable above background (<0.3% of *Bz'3*) in assays of the reference recessive allele (*bz-r*) or a deletion of the *bz* locus (*bz-X2*).

[c] CRM: the amount of UFGT-specific cross-reacting material present in crude extracts of each tissue.

[d] The thermal inactivation rate at 55° of partially purified UFGT was determined and the half-life was calculated from the data.

tion removed the terminal two bp of the 5′ 13 bp inverted repeat.

UFGT activities and CRM levels: At maturity, crude extracts of *bz-m13* endosperms contain approximately 5% of the level of UFGT activity observed in crude extracts of *Bz'3* endosperms, the functional *Bz* control (Table 1). UFGT activities are quite stable over time in the mature dry seed. Once extracted the UFGTs produced by the *bz-m13* series of alleles are unstable as compared with *Bz'3* and other functional *Bz* alleles' UFGTs (see below). Therefore, to optimize comparisons of genetic differences in enzymatic activity, we conducted all assays on freshly made crude extracts, and not on 30–60% ammonium sulfate fractions, as done previously (KLEIN and NELSON 1983).

The endosperm UFGT activities of *CS5* and *CS6* were similar to that of *bz-m13* (Table 1). *CS3* and *CS9* had increased levels of endosperm UFGT activity as compared with *bz-m13* (37 and 67% of Bz'3 UFGT activity, respectively). *CS12* endosperm UFGT activity is reduced as compared with *bz-m13*, to the extent that it is not reproducibly detectable in this tissue. It has been previously shown that the reduction in UFGT activity in mature endosperms of *bz-m13* as compared with *BzMcC* is not due to a change in the developmental timing of *bz* expression (KLEIN and NELSON 1983). We found this also to be true for the CSs of *bz-m13* included in this study (data not shown).

Although the stocks used in this study are near-isogenic, residual heterogeneity might have been responsible for some of the observed differences in endosperm UFGT activity. Therefore, as a second test of allelic differences we assayed husk UFGT activities in stocks homozygous for *B* and *P1* and the various *bz* alleles. The relative differences in husk UFGT activity observed among *bz-m13* and its CSs closely paralleled observed differences in endosperm UFGT activity (Table 1). UFGT activities of *bz-m13* and its CSs tended to be higher relative to *Bz'3* in husk tissues versus endosperm tissues. As an example, where we recover 7% or less of *Bz'3* activity in the endosperms of *bz-m13*, *CS5*, and *CS6*, we recovered from 13 to 20% of *Bz'3* activity in husk crude extracts. In addition, where we could not reproducibly detect UFGT activity in endosperm crude extracts of *CS12*, we can consistently detect UFGT activity in crude extracts of husk tissue of this mutant. This activity is reduced as compared with *bz-m13* (25 vs. 128 units/mg protein, respectively), confirming the difference between these two alleles observed in endosperm tissues.

CRM levels in the endosperm crude extracts were closely proportional to endosperm UFGT activity in all cases (Table 1). At the time of this study, the only anti-UFGT serum available was raised against partially purified *Bz-W22* endosperm UFGT. In attempting to measure CRM levels in husk extracts, we found that this anti-endosperm UFGT serum had a very low affinity for husk UFGT (data not shown). We therefore made no further attempts to measure CRM levels in crude husk extracts. As will be discussed in the next section, endosperm and husk UFGTs from a given allele also differ in their thermal stability. These tissue-specific differences in the properties of UFGT require further study.

UFGT thermal stability profiles: Thermal stability profiles were determined using endosperm and husk UFGTs obtained in a 30–60% ammonium sulfate fraction, dialyzed overnight to equilibrate salt concentrations, and adjusted against the same dialysis buffer to a constant total protein concentration. No data are given for *CS12* since UFGT activity was too low to accurately measure thermal denaturation. The half-lives at 55° of UFGT activities were calculated and are given in Table 1.

The thermal stability of *bz-m13* and CS endosperm UFGTs were similar, with half-lives at 55° ranging from 3.1 to 3.6 min. Their thermal stabilities differed from those of *Bz'3* and *BzMcC2*, whose endosperm UFGTs had half-lives at 55° of 9.9 and 7.9 min, respectively. In all cases, each allele's husk UFGT tended to be more stable than its endosperm UFGT. As observed with the endosperm assays, the thermal

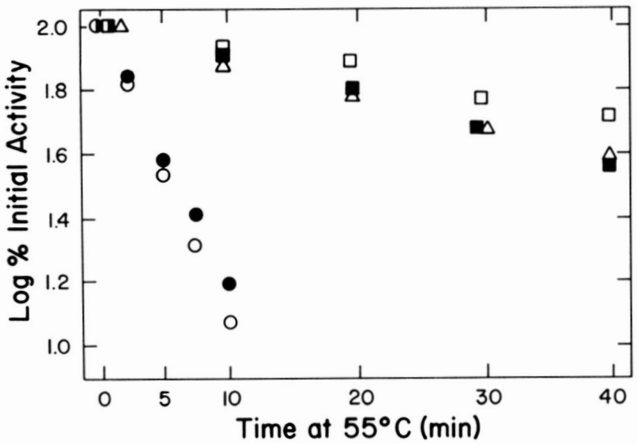

FIGURE 2.—Thermal inactivation profiles of UFGTs isolated from husk tissue of *bz-m13* (○), *CS9* (●), *Bz′3* (□), and mixtures of *bz-m13* and *Bz′3* (■), and *CS9* and *Bz′3* (△). Aliquots of enzyme preparations that were ammonium sulfate fractionated, dialyzed and adjusted to equivalent levels of total protein were incubated at 55° for the indicated times and assayed for remaining UFGT activity using standard methods. For the mixing experiments, aliquots of the given enzyme preparations that were of equal volume and total protein were thoroughly mixed and assayed for thermal inactivation rates.

stabilities of *bz-m13* and CS husk UFGTs were similar (half-lives at 55° ranging from 3.4 to 5.5 min), and less stable than *Bz′3* husk UFGT (44.5 min at 55°).

Mixing experiments were conducted to determine whether the relative thermal instability of *bz-m13* and *CS9* UFGTs as compared with *Bz′3* UFGT is due to an intrinsic difference in their UFGTs or due to an extrinsic factor present in their crude extracts. An aliquot of *bz-m13* or *CS9* husk extract, containing an equivalent amount of total protein, was mixed with an aliquot of *Bz′3* husk extract, and the UFGT thermal stability profile of the mixture was determined. Aliquots of extracts of the mutant alleles imparted no significant instability to the UFGT in extracts of *Bz′3* (Figure 2). This indicates that no extrinsic factor is responsible for the observed differences in thermal stability. An experiment using *Bz-W22* husk crude extract instead of *Bz′3* provided similar results (data not shown).

RNA analyses: Blot hybridization analyses of poly(A)$^+$ RNAs isolated from the husk tissue of plants homozygous for *bz-m13* or its CSs in the absence of an active *Spm* reveal that each of these alleles produce a *Bz*-specific RNA similar in size to that of the *Bz′3* mRNA (1.8 kb, Figure 3a). In addition, the *bz-m13* series of alleles produce either one (*CS3* and *CS9*) or two (*bz-m13*, *CS5*, *CS6* and *CS12*) RNA species of larger size not found in the blots of *Bz′3* poly(A)$^+$ RNA. Of these additional RNA species, the largest species in each case corresponds in size to that expected if one were to add the size of the particular *dSpm* insert to that of the *Bz′3* mRNA. The RNA species of intermediate size found in *bz-m13*, *CS5*,

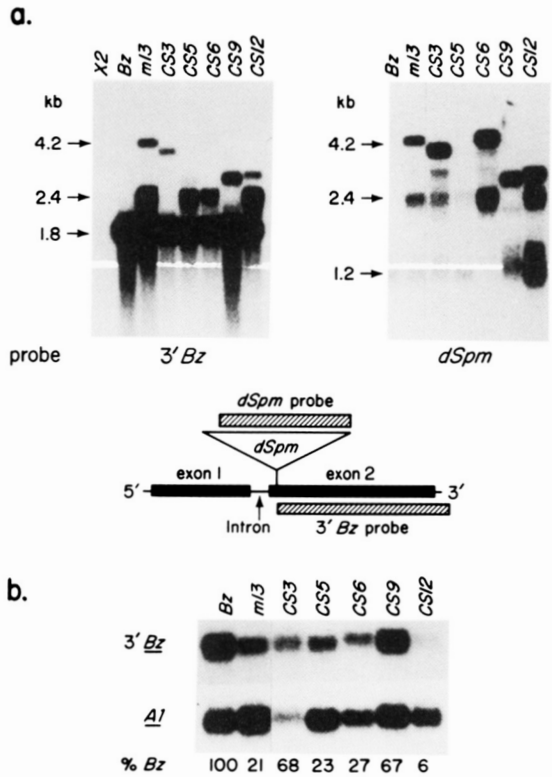

FIGURE 3.—Northern blot analysis of poly(A)$^+$ RNAs encoded by *bz-m13* and its change in state derivatives. Poly(A)$^+$ RNAs were isolated from husk tissue of plants homozygous for the indicated alleles of the *bz* locus in the absence of an active *Spm*: x2, *bz-x2*; Bz, *Bz′3*; m13, *bz-m13*; CS3, CS5 etc., *bz-m13 CS3*, *bz-m13 CS5*, etc. a) The poly(A)$^+$ RNAs were fractionated in formaldehyde-containing 1.2% agarose gels, transferred to nitrocellulose filters, and hybridized to the ^{32}P-labeled probes indicated at the bottom of the autoradiograms. The size of the RNAs given on the left were calculated on the basis of the mobility of the RNA size markers. b) Quantitation, relative to the internal levels of *a* RNA, of the levels of the 1.8 kb RNAs that hybridize to the 3′ *Bz* probe in (a). An autoradiogram of the filter in (a), hybridized to the 3′ *Bz* probe indicated at the bottom of (a), was produced using a shorter exposure than that used in (a). Only the bands of the 1.8-kb RNAs are shown. The filter was stripped of the 3′ *Bz* probe and rehybridized with the ^{32}P-labeled plasmid pALC2, which contains the transcription unit of the *a* locus. The autoradiogram of the reprobed filter shows only one band of RNA hybridizing to the *a* probe in each lane, as indicated in (b). The amounts of probe hybridizing to each band was measured with a densitometer. The levels of 1.8-kb RNAs were normalized to the levels of RNA hybridizing to the *a* probe, and expressed as a percentage of the normalized level of *Bz′3* RNA, given at the bottom of (b).

CS6, and *CS12*, but not found in *CS3* and *CS9*, are similar in size (approximately 2.4 kb). The larger RNA species hybridize to both the *Bz* sequence 3′ of the *dSpm* insertion and to the *dSpm* sequence, whereas the 1.8 kb RNA bands only hybridize to 3′ *Bz* sequence.

An initial inspection of an autoradiogram representing a shorter exposure than that in Figure 3a indicated that the 1.8 kb RNA levels were proportional to the levels of UFGT activity found in each state of *bz-m13* (Table 1). We required an internal

control to best assay the above correspondence since husk tissue samples may differ slightly in developmental state, and variable levels of poly(A)$^+$ RNA are recovered from any given preparation. The filter in Figure 3A was stripped of *Bz* probe, and hybridized with the plasmid pALC2, which contains the entire transcriptional unit of the *a* gene (SCHWARZ-SOMMER *et al.* 1985), an anthocyanin pathway structural gene. The autoradiograms of the Northern blots probed with *Bz* sequence, and reprobed with *a* (Figure 3b), were scanned with a densitometer. The levels of the 1.8-kb RNA, normalized relative to internal levels of *a* mRNA and expressed as a percent of *Bz'3*, are given in Figure 3B. The results clearly demonstrate that these levels are proportional to the levels of husk UFGT activities observed in each allele (Table 1).

We have previously shown (KIM *et al.* 1987) that a splicing event utilizing the donor splice site of the single *bz* intron and an acceptor splice site (AS1) in the *dSpm*'s 13-bp terminal inverted repeat can produce the 1.8-kb RNAs observed in Figure 3a. We next hypothesized that the 2.4 kb RNAs found in *bz-m13*, *CS5*, *CS6*, and *CS12*, are the products of a splicing event which utilizes a second, alternative acceptor splice site (AS2) located within the *dSpm* sequence upstream of AS1. The difference in size between the 1.8- and 2.4-kb RNAs (0.6 kb) led us to search the corresponding region of the *dSpm* for such a site. We therefore conducted an S1 nuclease protection experiment utilizing as probe a 706-bp 5′ end-labeled *Sph*I-*Sal*I fragment which encompasses this region (Figure 4). The results in Figure 4 show that *bz-m13* RNA protects a fragment of 363 to 367 bp. This would place AS2 about 627 bp upstream of AS1. A sequence which has the obligatory AG dinucleotide and 11 of 16 bp homologous to the consensus plant acceptor site sequence (BROWN 1986) was identified at this position (Figure 5).

The deletions that gave rise to the two CSs which have an increased level of UFGT activity relative to *bz-m13*, *CS3* and *CS9*, removed similar portions of the *dSpm* sequence, and it is these two CSs that lack the intermediate 2.4-kb RNA. In the case of *CS9*, the deletion removed AS2, whereas in *CS3* the deletion removed approximately 400 bp between AS1 and AS2.

A 1.2-kb RNA which hybridizes to the *dSpm* probe is also detected in the Northern blots (Figure 3A). This RNA differs from the higher molecular weight RNAs which hybridize to the *dSpm* probe in two ways: it does not hybridize to either 3′ (Figure 3A) or 5′ (data not shown) *Bz* probes; it is detected in *Bz'3* poly(A)$^+$ RNA as well as in the poly(A)$^+$ RNAs isolated from the *bz-m13* series of alleles. This 1.2-kb RNA is much more abundant in *CS12* poly(A)$^+$ RNA than any of the other alleles tested.

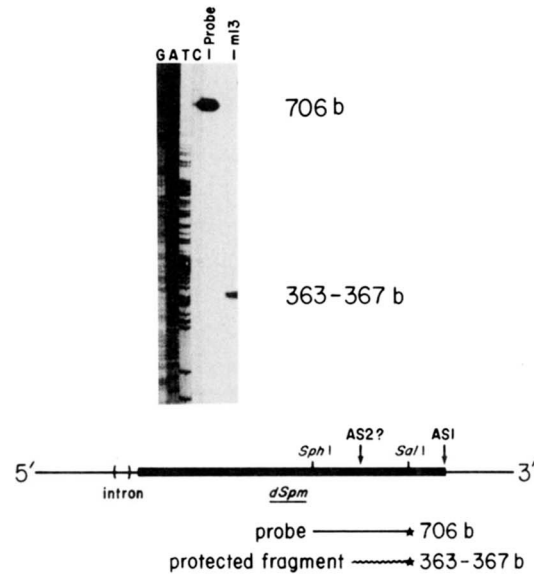

FIGURE 4.—S1 nuclease mapping of the alternative acceptor splice site (indicated as AS2 in the fiture) presumably located 5′ to the acceptor splice site located in the *dSpm*'s terminal inverted repeat (indicated as AS1 in the figure). The 5′-end-labeled *Sph*I/*Sal*I fragment shown in the diagram was hybridized to poly(A)$^+$ RNAs isolated from *bz-m13* (m13), treated with S1 nuclease, and fractionated in a 5% urea-polyacrylamide gel. DNA sequence reactions were used as size markers.

***dSpm* germinal excision rates:** The deletions which gave rise to these CSs of *bz-m13* occurred in the presence of *Spm-s* activity. Their subsequent germinal stability in the presence of *Spm-s* activity is relevant to an evaluation of their evolutionary significance. Therefore, to further characterize the effects of these deletions we estimated their germinal excision rates in response to *Spm-s*. The large number of stable bz′ and Bz′ derivatives produced by *bz-m13* in the presence of *Spm-s* has been shown to result from *Spm-s* induced excision of the *dSpm* insert (SCHIEFELBEIN *et al.* 1988). Estimated germinal excision rates in the presence of *Spm-s* were determined by quantitating the frequency of bz′ and Bz′ derivatives observed in reciprocal crosses with a *Spm-s* tester stock (Table 2).

The CSs representing relatively large deletions of the *dSpm* insertion (*CS3*, *CS5*, *CS9*, and *CS12*) produce few stable *Bz′* and *bz′* derivatives in the presence of an active *Spm-s*. Individual test crosses occasionally yield no recovered derivatives. Where detected, typical estimates of germinal excision rates ranged from less than 1% to 2%. *CS6* appears to produce slightly higher germinal excision rates (3 and 7% in female and male gametes, respectively, in a typical case). In comparison, a representative test of the initial insertion mutation *bz-m13* produced 53 and 71% stable derivatives in female and male gametes, respectively.

In theory all progeny kernels from these test-crosses should contain at least one active *Spm-s*. In practice a variable number of kernels on a given testcross ear are fully pigmented and contain an unchanged *bz-m13*

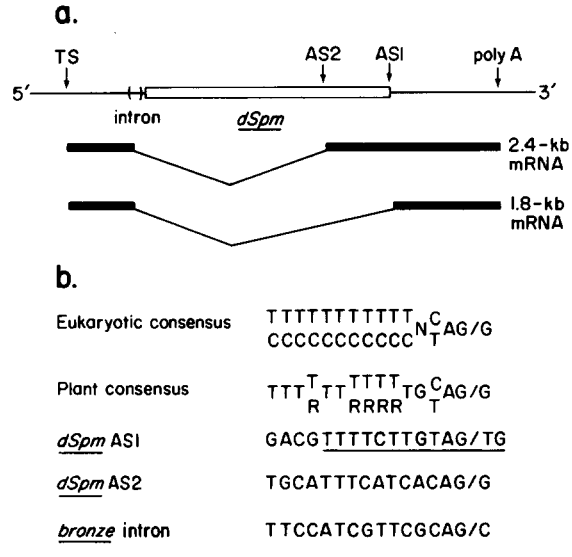

FIGURE 5.—Proposed structure of the *bz-m13* mRNAs, and comparison of the acceptor splice site sequences that generate these proposed mRNAs with the consensus eukaryotic and plant acceptor site sequences. a) The proposed structures of the 2.4-kb and 1.8-kb mRNAs observed in *bz-m13* and several of its CSs. AS1 refers to the acceptor splice site located within the terminal inverted repeat (KIM *et al.* 1987). AS2 refers to the alternative acceptor site located 627 bp 5′ to the AS1 splice site. TS, transcription start site; poly A, polyadenylation site. b) Comparison of the sequences of the AS1 and AS2 splice sites with the consensus sequences for eukaryotic (MOUNT 1982) and plant (BROWN 1986) acceptor sites. The 13-bp terminal inverted repeat of the *Spm* family that contains the AS1 splice site is underlined. The acceptor site sequence of the *bz* intron (FURTEK 1986) is shown for comparative purposes. R = A or G; N = A, C, G, or T; slash (/) = the intron-exon junction. When two bases are shown in the same position, the upper base is observed more frequently.

allele in the absence of *Spm-s* activity (NELSON and KLEIN 1984; Table 2). The initial state of *bz-m13*, in the presence of *Spm-s*, yields numerous stable *Bz′* derivatives, and only a small fraction of kernels displaying full anthocyanin pigmentation represent an unchanged *bz-m13* in the absence of *Spm-s*. The *CSs*, on the other hand, produce few stable *Bz′* derivatives, and subsequent progeny tests reveal that most fully pigmented kernels on test cross ears contain unchanged CSs in the absence of *Spm-s* activity.

DISCUSSION

The relationship between UFGT activity and steady-state RNA levels: We found that two CSs, *CS5* and *CS6*, have similar UFGT activities to that of the initial insertion mutation *bz-m13*. Two CSs, *CS3* and *CS9*, have increased UFGT activities, and the fifth CS, *CS12*, has a decreased UFGT activity. The close relationship between CRM levels and UFGT activity suggests that the differences in UFGT activity in the mature dry kernels were primarily due to differences in the accumulation of UFGT protein, and not due to large differences in the catalytic properties of a given mutant UFGT. Also, observed differences in UFGT activity could not be attributed to differences in the developmental timing of expression or to differences in thermal stability.

TABLE 2

Estimated germinal excision rates of the *bz-m13* alleles' *dSpm* insertions in the presence of an active *Spm-s*

Allele[a]	Gametes tested	Total kernels	Progeny kernel genotypes[b]					Estimated % germinal excision[c]
			bz-m13 allele				*Sh bz′* and *Sh bz*	
			sh bz	*+Spm-s*	*−Spm-s*	*Bz′*		
bz-m13	♂	280	139	41	0	33	67 (3)	71
	♀	216	111	45	3	19	38 (2)	53
CS3	♂	243	112	126	5	0	0	0
	♀	390	191	176	15	0	8 (4)	2
CS5	♂	232	125	101	1	1	4 (2)	1
	♀	254	116	131	3	1	3 (3)	1
CS6	♂	310	115	146	4	0	15 (3)	7
	♀	332	164	159	1	0	8 (3)	3
CS9	♂	256	132	122	1	1		1
	♀	259	138	120	1	0		0
CS12	♂	264	121	139	0	0	4 (3)	1
	♀	418	218	193	4	0	3 (3)	0

Plants of the genotype *Sh bz-m13/sh bz-r*; + *Spm-s* or *Sh bz-m13 "CS"/sh bz-r*; *+Spm-s* were used as both males and females in crosses with a tester stock of the genotype *sh bz-r/sh bz-r*; *+Spm-s*. Typical data from crosses of each allele are given.

[a] Allele: *bz-m13*, the initial state; *CS3*, *bz-m13 CS3*; *CS5*, *bz-m13 CS5* etc. All *bz-m13* alleles are linked to *Sh*, a *nonshrunken* allele of the *shrunken* locus, with the exception of *CS9*, which is linked to *sh*, a *shrunken* allele.

[b] Kernel phenotypes: *sh bz*, *shrunken bronze*; *bz-m13* allele + *Spm-s*, variegated; *bz-m13* allele *−Spm-s*, nonsectored purple; *Bz′*, nonsectored purple; *Sh bz′* and *Sh bz*, nonshrunken bronze. The number in the parentheses under "*Sh bz′* and *Sh bz*" are estimates of the numbers of *Sh bz* kernels expected based on the assumption of 2% recombination between *sh* and *bz*. The linkage with *Sh* and *sh* is used here only to distinguish between *sh bz/sh bz* and *Sh bz′/sh bz* progeny. The *CS9* allele is linked to *sh*, so this distinction cannot be made in this case.

[c] The estimated germinal excision rates are calcualted as 100 × the sum of (1) the excess of *Sh bz* kernels (assumed to be *Sh bz′*) over the expected number resulting from recombination between *sh* and *bz* and (2) the number of *Bz′* kernels divided by the sum of (1) and (2) plus the number of *bz-m13* + and − Spm-s kernels.

RNA analyses indicate that in all alleles transcription proceeds through the *dSpm* insert thus producing the largest *Bz*-specific RNA. We hypothesize that the pre-mRNA processing event using the AS1 site as illustrated in Figure 5a is responsible for the production of the mRNA whose translation produces the functional UFGT found in *bz-m13* and the other CSs. This hypothesis is supported by the close relationship between the level of the 1.8-kb mRNA and the level of UFGT activity typical of each allele.

Alternative pre-mRNA processing events which alter the steady-state level of the 1.8-kb RNA appear to be responsible for the differences in UFGT activity observed between *bz-m13* and some of its CSs. Processing events utilizing AS2 result in an RNA containing *dSpm* sequence. This *dSpm* sequence contains in-frame translation termination codons, which would upon translation result in a presumably truncated,

nonfunctional UFGT protein (KIM 1987). When deletions remove AS2, as in the case of *CS9*, competition of AS2 with AS1 cannot occur, and the prevalent splicing event is that which utilizes AS1.

The deletion found within the *dSpm* insert in *CS3* did not remove AS2, instead it removed approximately 400 bp of sequence between AS1 and AS2. If AS2 were utilized during processing of *CS3* RNA, a 2.1-kb band would be produced. Since no such RNA has been detected, the 400 bp deletion in *CS3* altered the utilization of the AS2 site.

Other factors may contribute to the differences in UFGT activity and 1.8-kb RNA levels among *bz-m13* and these CSs. Transposable element insertions may affect transcription rates and not RNA processing (ROWLAND and STROMMER 1985). Differences in transcription rate may contribute in part to the observed differences in *bz* expression. The deletions in the CSs may alter RNA stability, or alter the formation of the lariat structure critical to the splicing reaction by deleting or changing the position of branch points (GREEN 1986). The deletion in *CS9* has removed the promoter of *Spm*'s gene 1 transcript located within the SRR and the GC rich sequence proximal to *Spm*'s 5′ SRR. These two types of sequences may influence *bz* transcription rate. Activity of the *Spm* gene 1 promoter would produce transcripts containing *dSpm* sequence complementary, or antisense, to the *dSpm* sequence in transcripts resulting from *bz* promoter activity. Complementary transcripts may result in an antisense RNA interaction (ECKER and DAVIS 1986), reducing net *bz* expression in those states retaining the promoter.

At present we do not understand the cause of the reduction in *bz* expression in *CS12* as compared with *bz-m13*. The deletion found in *CS12* may be responsible via an unknown mechanism. Alternatively, the relative abundance of the 1.2-kb *dSpm*-specific RNA in *CS12* poly(A)$^+$ RNA may be responsible. Perhaps this RNA is antisense to the *dSpm* sequence in *CS12*'s primary transcript.

Evolutionary relationships between transposable elements and introns: There are two views, often characterized as being diametrically opposed, on the origin and evolution of introns (CAVALIER-SMITH 1985; GREEN 1986; SHARP 1985). The first view holds that ancestral eukaryotic genes were discontinuous, and that splicing evolved to bring coding sequences together. The second view holds that introns arose by insertion of transposable elements. CAVALIER-SMITH (1985) proposed that certain introns might have originated as "defective transposons in which the RNA-splicing mechanism evolved from preexisting DNA splicing enzymes specific for their termini." Arguing against this hypothesis, SHARP (1985) noted that no known transposable element has splice sites at its termini. Our previous report (KIM *et al.* 1987) documented the presence of an acceptor splice site (AS1) in the terminal inverted repeat of *dSpm* elements.

Here we show that the initial insertion mutation *bz-m13* and several of its derivatives also contain an alternative acceptor site (AS2 in Figure 5a) internal to AS1. Members of the *Activator-Dissociation* (*Ac-Ds*) family of maize transposable elements also contain splice sites in their minus strand adjacent to their terminal inverted repeats and not associated with any known transposable element gene. The *wx-m9* allele of the *waxy* locus in maize contains a 4.3-kb *Dissociation* (*Ds*) element inserted in *wx*'s 10th exon (WESSLER, BARAN and VARAGONA 1987). This *Ds* element represents a deletion derivative of the *Activator* (*Ac*) transposable element, is inserted in the *wx* gene in opposite orientation in terms of their respective directions of transcription and contains a series of four putative 5′ donor sites in its minus strand within 30 bp of its 3′ terminal inverted repeat. In the absence of *Ac* activity, transcription proceeds through the *Ds* insertion in *wx-m9*. Nearly all of the *Ds* sequence in the pre-mRNA is removed during pre-mRNA processing in a splicing event using one of the four 5′ donor splice sites in the *Ds* termini and a cryptic acceptor splice site in *wx* sequence 3′ of the insertion. A similar splicing event removes *Ds* sequence from transcripts of the *Adh1-FM335* allele of the maize *ADH1* gene (DENNIS *et al.* 1988).

In both cases the donor site provided by the *Ds* insertion is internal to *Ds*'s terminal inverted repeat. Thus the *Ac-Ds* family contains a series of alternative donor sites in its minus strand adjacent to its terminus, and the *Spm-dSpm* family contain at least two acceptor splice sites in its minus strand within and internal to its terminus. These splice sites allow for the removal of element sequence from read-through transcripts of genes in which these elements are inserted in exons in opposite orientation in terms of their respective directions of transcription. This splicing mechanism may serve to reduce the impact of transposable element insertion on gene expression (KIM *et al.* 1987; WESSLER, BARAN and VARAGONA 1987).

Clearly, the insertion of a maize transposable element in and of itself can alter the intervening sequence of a gene. Here we document a sequence of events which begins with the insertion of a transposable element and leads to novel and stable intron structures. First, a 2.2-kb *dSpm* insertion in the second exon of the *Bz-McC2* allele occurred in the presence of *Spm-s*. Next, *Spm* catalyzed deletions within the 2.2 kb *dSpm* both stabilized the remnant insertion, and in at least one case removed an alternative acceptor splice site (AS2) within the *dSpm*. Absence of *Spm-s* activity in a small fraction of progeny in subsequent generations frees these progeny of *Spm*'s *trans*-acting

effects. In the case where the deletion removed AS2, the *dSpm* sequence in the pre-mRNA is efficiently removed as part of a novel intron, producing near wild-type levels of an mRNA which upon translation produces significant quantities of functional protein.

The authors would like to thank ANITA KLEIN for assistance with the UFGT activity assay and for providing UFGT-specific antisera, DOUGLAS FURTEK for helpful discussions, ZSUZSANNA SCHWARZ-SOMMER for the *A* gene clone, Steven Sickler for Assistance in the laboratory, RUSSEL HUSSETH for assistance in the field, and SUSAN WESSLER for constructive criticism of the manuscript. This is Paper No. 3008 from the Laboratory of Genetics, University of Wisconsin-Madison. The research was supported by the College of Agriculture and Life Sciences and by grant DCB-8507895 from the National Science Foundation.

LITERATURE CITED

BERK, A. J., and P. A. SHARP, 1977 Sizing and mapping of early adenovirus mRNAs by gel electrophoresis of S1 and endonuclease digested hybrids. Cell **12:** 721–732.

BROWN, J. W. S., 1986 A catalogue of splice junction and putative branch point sequences from plant introns. Nucleic Acids Res. **14:** 9549–9559.

CANTOR, C. R., and P. R. SCHIMMEL, 1980 *Biophysical Chemistry.* W. H. Freeman, San Francisco.

CAVALIER-SMITH, T., 1985 Selfish DNA and the origin of introns. Nature **315:** 283–284.

DENNIS, E. S., M. M. SACHS, W. L. GERLACH, I. BEACH and W. J. PEACOCK, 1988 The *Ds1* transposable element acts as an intron in the mutant allele *Adh1-Fm335* and is spliced from the message. Nucleic Acids Res. **16:** 3815–3828.

DOONER, H. K., and O. E. NELSON, 1977a Genetic control of UDPglucose:flavonoid 3-*O*-glucosyltransferase in the endosperm of maize. Biochem. Genet. **15:** 509–519.

DOONER, K., and O. E. NELSON, 1977b Controlling element-induced alterations in UDPglucose:flavonoid glucosyltransferase, the enzyme specified by the *bronze* locus in maize. Proc. Natl. Acad. Sci. USA **74:** 5623–5627.

ECKER, J. R., and R. W. DAVIS, 1986 Inhibition of gene expression in plant cells by expression of antisense RNA. Proc. Natl. Acad. Sci. USA **83:** 5372–5376.

FAVALORO, J. R., R. TREISMAN and R. KAMEN, 1980 Transcription maps of polyoma virus-specific RNA: analysis by 2-dimensional nuclease S1 gel mapping. Methods Enzymol. **65:** 718–749.

FEDOROFF, N., 1983 Controlling elements in maize, pp. 1–63 in *Mobile Genetic Elements*, edited by J. SHAPIRO. Academic Press, New York.

FURTEK, D. B., 1986 Cloning and sequence analysis of the *bronze* locus in maize: location of transposable element insertions and comparison of two wild type alleles. Ph.D. thesis, University of Wisconsin-Madison.

GERATS, A. G. M., J. BUSSARD, E. H. COE and R. LARSON, 1984 Influence of *B* and *P1* on UDPG:flavonoid-3-*O*-glucosyltransferase in *Zea mays* L. Biochem. Genet. **22:** 1161–1169.

GREEN, M. R. 1986 Pre-mRNA splicing. Annu. Rev. Genet. **20:** 671–708.

KIM, H-Y., 1987 Molecular characterization of a functional mutation caused by insertion of a defective *Suppressor-mutator* transposable element in the *bz-1* locus of maize. Ph.D. thesis, University of Wisconsin-Madison.

KIM, H-Y., J. W. SCHIEFELBEIN, V. RABOY, D. B. FURTEK and O. E. NELSON, 1987 RNA splicing permits expression of a maize gene with a defective Suppressor-mutator transposable element insertion in an exon. Proc. Natl. Acad. Sci. USA **84:** 5863–5867.

KLEIN, A. S., and O. E. NELSON, 1983 Biochemical consequences of the insertion of a suppressor-mutator (*Spm*) receptor at the bronze-1 locus in maize. Proc. Natl. Acad. Sci. USA **80:** 7591–7595.

LARSON, R. L., and E. H. COE, 1977 Gene dependent flavonoid glucosyltransferase in maize. Biochem. Genet. **15:** 153–156.

MASSON, P., R. SUROSKY, J. A. KINGSBURY and N. V. FEDOROFF, 1987 Genetic and molecular analysis of the *Spm*-dependent *a-m2* alleles of the maize *a* locus. Genetics **117:** 117–137.

MCCLINTOCK, B., 1954 Mutations in maize and chromosomal aberrations in Neurospora. Carnegie Inst. Wash. Year Book **53:** 254–260.

MCCLINTOCK, B., 1955 Controlled mutation in maize. Carnegie Inst. Wash. Year Book **54:** 245–255.

MCCLINTOCK, B., 1968 The states of a gene locus in maize. Carnegie Inst. Wash. Year Book **66:** 664–672.

MOUNT, S. M., 1982 A catalogue of splice junction sequences. Nucleic Acids Res. **10:** 459–472.

NELSON, O. E., and A. S. KLEIN, 1984 Characterization of an *Spm*-controlled bronze-mutable allele in maize. Genetics **106:** 769–779.

PEREIRA, A., H. CUYPERS, A. GIERL, Z. SCHWARZ-SOMMER and H. SAEDLER, 1986 Molecular analysis of the *En/Spm* transposable element system of *Zea mays*. EMBO J. **5:** 835–841.

PETERSON, P. A., 1953 A mutable pale green locus in maize. Genetics **38:** 682.

PETERSON, P. A., 1960 The pale green mutable system in maize. Genetics **45:** 115–133.

PETERSON, P. A., 1965 The relationship between the *Spm* and *En* control systems in maize. Am. Nat. **99:** 391–398.

ROWLAND, L. J., and J. N. STROMMER, 1985 Insertion of an unstable element in an intervening sequence of maize *Adh1* effects transcription but not processing. Proc. Natl. Acad. Sci. USA **82:** 2875–2879.

SCHIEFELBEIN, J. W., 1987 Molecular characterization of mutations at the maize *bronze-1* locus caused by the *Ac-Ds* and *Spm-dSpm* transposable element families. Ph.D. thesis, University of Wisconsin-Madison.

SCHIEFELBEIN, J. W., V. RABOY, N. V. FEDOROFF and O. E. NELSON, 1985 Deletions within a defective Suppressor-mutator in maize affect the frequency and developmental timing of its excision from the bronze locus. Proc. Natl. Acad. Sci. USA **82:** 4783–4787.

SCHIEFELBEIN, J. W., V. RABOY, H.-Y. KIM and O. E. NELSON, 1988 Molecular characterization of *Suppressor-mutator* (*Spm*)-induced mutations at the *bronze-1* locus in maize: the *bz-m13* alleles, pp. 261–278 in *Plant Transposable Elements*, edited by O. E. NELSON. Plenum Press, New York.

SCHWARZ-SOMMER, Z., A. GIERL, R. B. KLOSGEN, U. WIENAND, P. A. PETERSON and H. SAEDLER, 1984 The *Spm* (*En*) transposable element controls excision of a 2-kb DNA insert at the *wx-m8* allele of *Zea mays*. EMBO J. **3:** 1021–1028.

SHARP, P. A., 1985 On the origin of messenger RNA precursors. Cell **42:** 397–400.

SIMON, R., and P. STARLINGER, 1987 Transposable element *Ds2* of *Zea mays* influences polyadenylation and splice site selection. Mol. Gen. Genet. **209:** 198–199.

WESSLER, S. R., G. BARAN and M. VARAGONA, 1987 The maize transposable element *Ds* is spliced from RNA. Science **237:** 916–918.

Communicating editor: S. D. TANKSLEY